

Ternary System $\text{H}_2\text{O}-\text{CO}_2-\text{NaCl}$ at High $T-P$ Parameters: An Empirical Mixing Model

L. Ya. Aranovich^{a,b}, I. V. Zakirov^b, N. G. Sretenskaya^b, and T. V. Gerya^b

^a Institute of the Geology of Ore Deposits, Petrography, Mineralogy, and Geochemistry (IGEM), Russian Academy of Sciences,
Staromonetnyi per. 35, Moscow, 109017 Russia

e-mail: lyaranov@igem.ru

^b Institute of Experimental Mineralogy, Russian Academy of Sciences, Institutskii pr. 4, Chernogolovka,
Moscow oblast, 142432 Russia

e-mail: ziv@iem.ac.ru

Received November 26, 2008

Abstract—New experimental data on the solubility of NaCl in gaseous CO₂ were obtained at pressures (P) of 30–70 MPa and temperatures of 623 and 673 K on experimental equipment making possible to sample a portion of the gas in the course of the experiment. The new measures have demonstrated that the NaCl solubility increases with increasing temperature (T) and pressure and is approximately four to five orders of magnitude higher than the saturated vapor pressure of NaCl at the corresponding temperature. The paper also reports newly obtained experimental data on the equilibrium conditions of the reaction of talc decomposition into enstatite and quartz at a variable H₂O/NaCl ratio in the fluid. The results of the experiments validate the empirical equations previously suggested for H₂O and NaCl activities in concentrated aqueous salt solutions that can be used in describing silica-saturated fluids at high $T-P$ parameters. A new empirical equation is suggested for the Gibbs free mixing energy in the H₂O–CO₂–NaCl ternary system, with the parameters of the equation calibrated against experimental data on phase equilibria in marginal binary systems and on the location of the boundary of the region of homogeneous three-component fluid according to data on synthetic fluid inclusions in quartz.

DOI: 10.1134/S0016702910050022

INTRODUCTION

Processes involving the action of fluids are widespread in the earth's lithosphere. The degassing of internal shells of the earth resulted in elevated concentrations of volatile, low-melting, and radioactive elements in the outer zones of the planet and caused its more stable stratification. The re-involvement of these components in endogenic processes in subduction zones is now thought to be one of the predominant mechanisms maintaining the evolution of continents. Large-scale crust-building processes, such as regional metamorphism, that were commonly regarded, particularly by Western researchers, as proceeding in closed systems (with the only exception of the participation of water and carbon dioxide in these processes), are now more and more often considered to be metasomatic in their essence. They provide a record for the interaction of the rocks with much fluids of external (with respect to the rocks) provenance [1–7]. One of the most important results of these investigations was the conclusion that alkalis are widely involved in processes of high-grade regional metamorphism (behave as perfectly mobile components, according to Korzhinskii [2]). Experimental results on synthetic fluid inclusions [8–10], interpretations of phase relations in high-temperature calc-silicate rocks [11, 12], and the detection of high-temperature salts in the interstitial space of high-grade metamorphic rocks

[13, 14] definitely testify that multicomponent fluids (H₂O–CO₂ + strong electrolyte) should play an important part in processes forming metamorphic mineral assemblages. Such fluids can be provisionally approximated by the ternary system H₂O–CO₂–NaCl [4, 15]. In spite of the obvious importance of this system for the interpretation of phase relations in metamorphic and magmatic rocks, the thermodynamics of the system is known still inadequately poorly, particularly at high pressures (P), temperatures (T), and salt concentrations.

This publication presents our measurements of the NaCl solubility in gaseous CO₂ conducted at 623 and 673 K, under pressures of 35–70 MPa. The experiments were carried out in experimental equipment of our original design, which allows the researcher to sample the gaseous phase at the parameters of the experiments [16]. These results are compared with the values of solubility calculated by the equation of state suggested for the ternary system by Duan et al. [17]. The newly obtained experimental data were used to calculate parameters of an empirical equation for the mixing energy of CO₂ and NaCl in very strongly diluted salt solutions that can be applied in the thermodynamic description of the ternary system. We also report recently obtained experimental data on testing the applicability of the equations for the mixing energy in the binary system H₂O–NaCl to solu-

Table 1. Experimental data on NaCl solubility in gaseous CO₂

<i>P</i> , MPa	Mass <i>m</i> _{CO₂} (total), g	Mass <i>m</i> _{Na⁺} (in.), μg	Mass <i>m</i> _{CO₂} (in.), g
623 K			
33	27.8	0.46	5.64
33.3	27.9	0.47	5.67
54	39	3.80	7.92
54.6	41.5	3.60	8.43
54.2	41	3.90	8.33
53.6	40.8	3.70	8.29
56	44.5	4.48	9.04
55.6	44.1	4.50	8.96
55	44.2	4.25	8.98
56.4	44.5	4.45	9.04
56.7	44.8	4.65	9.10
65.2	47	6.80	9.55
65	46.6	6.72	9.47
64.9	47.2	6.83	9.59
65	46.8	6.88	9.51
673 K			
27.5	20.3	1.22	4.12
27	20	1.08	4.06
45	30.9	4.24	6.28
45.5	31.2	4.08	6.34
45.1	30	4.48	6.10
62.5	44.1	12.17	8.96
62.8	44.6	13.75	9.06
62.1	44	11.00	8.94
67.4	44.7	13.80	9.08
67.2	44	14.50	8.94

Note: *m*_{CO₂} (total) is the total CO₂ mass in the experiment, *m*_{Na⁺} is the Na⁺ concentration in the inner ampoule after the experiment, and *m*_{CO₂} (in.) is the mass of CO₂ in the inner ampoule.

tions saturated with respect to SiO₂. Based on equations for boundary binary systems and experimental data on the boundaries of the miscibility gap in the ternary system, we suggested a new equation for the free mixing energy of components in the ternary system H₂O–CO₂–NaCl.

BINARY SYSTEM NaCl–CO₂

Experimental data on the behavior of the boundary binary system NaCl–CO₂ are scarce. We are aware of only two publications devoted to this system: Grjotheim et al.

[18] measured the CO₂ solubility in NaCl melt at normal pressure, and Chou [19] published (in brief abstracts) data on the decrease in the halite melting temperature in the presence of CO₂ under a pressure of 200 MPa. As could be expected, the solubility at 1 atm is very low (roughly 5 × 10⁻⁶ mol of CO₂/mol of NaCl [18]). Because of this, the authors of all known equations of state for the ternary system [17, 20] had to calculate the mixing parameters for the boundary binary system NaCl–CO₂ based on experimental data on the ternary system, an approach known, however, to be an unreliable. In order to describe the

Table 2. Averaged values of the NaCl mole fraction in gaseous CO₂ and corresponding values of NaCl activity in the gaseous phase

T, K	P, MPa	X _{NaCl} × 10 ⁷	-RTln a _{NaCl, v} , J/mol*
623	33	1.569	10789
623	54	8.655	10868
623	56	9.520	10875
623	65	13.631	10908
673	27.5	5.680	9724
673	44	14.172	9790
673	62.5	25.965	9863
673	67	30.292	9881

* Calculated from data from the database [25] [see text for Eq. (2)].

binary system NaCl–CO₂ more reliably, the NaCl solubility in gaseous CO₂ was determined in [21] experimentally at 623 and 673 K and 35–75 MPa. The experimental equipment and methods are described in detail in [21]. The values of NaCl solubility in CO₂ measured in individual experiments are reported in Table 1. Inasmuch as it was impossible to load exactly equal amounts of CO₂ in each experiment, the pressures are slightly different in each of the “isobaric” experimental sets (Table 1).

Averaged values of NaCl solubility within the P-T range in question are listed in Table 2. As could be expected, these values are very low but are nevertheless

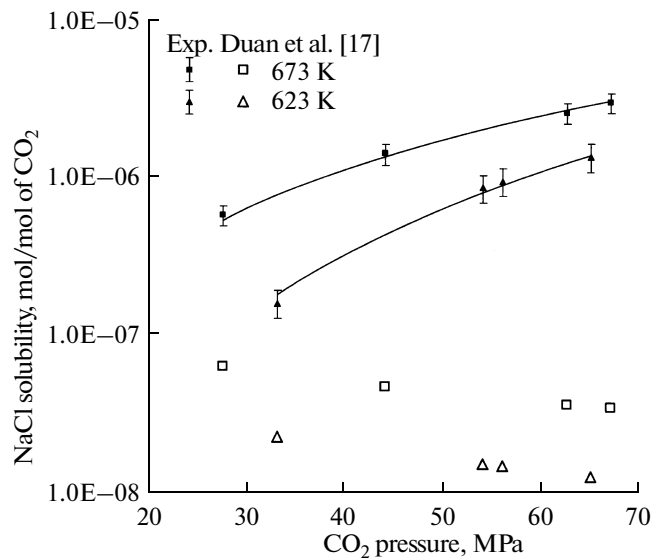


Fig. 1. Experimental values (solid symbols with error brackets) of NaCl solubility in gaseous CO₂ depending on CO₂ pressure. Continuous lines correspond to calculations by the DQF model [Eq. (3) in text]. Open symbols correspond to calculations by the equation of Duan et al. [17].

four to five orders of magnitude higher than the NaCl saturated vapor pressures calculated based on the data tabulated in [22] for corresponding temperatures (6.02 × 10⁻¹² at 623 K and 1.51 × 10⁻¹⁰ at 673 K). Our values are one to two orders of magnitude higher than the NaCl solubility calculated from the parameters of the CO₂–NaCl binary system used in the equation of state for the H₂O–CO₂–NaCl ternary system in [17] (Fig. 1). It should also be mentioned that, according to our experimental data, the solubility increases with both temperature and pressure, whereas Duan’s equation predicts that the solubility should decrease with increasing pressure (Fig. 1). An increase in the solubility with increasing pressure suggests that a weak chemical bond occurs between NaCl and CO₂ molecules in the high-temperature gas, an effect that can be caused by the interaction of the NaCl dipolar moment with the CO₂ quadrupole moment.

The condition of NaCl and CO₂ equilibrium is written as

$$\mu_{\text{NaCl}, s}^0 + RT \ln a_{\text{NaCl}, s} = \mu_{\text{NaCl}, v}^0 + RT \ln a_{\text{NaCl}, v}, \quad (1)$$

where $\mu_{\text{NaCl}, s}^0$ and $\mu_{\text{NaCl}, v}^0$ are the standard chemical potentials of NaCl in the solid (s) and gaseous (v) phases, respectively; and $a_{\text{NaCl}, s}$ and $a_{\text{NaCl}, v}$ are their activities. Solid NaCl is a pure phase, and its activity is equal to 1. According to the model often used in the description of the H₂O–NaCl boundary binary system [23, 24] and the ternary system H₂O–CO₂–NaCl [12], (metastable) NaCl melt is chosen as the standard state of NaCl in the gaseous phase. The standard chemical potentials of crystalline and molten NaCl were calculated as functions of pressure and temperature by the equations reported in the database [25]. The values of the difference

$$\mu_{\text{NaCl}, s}^0 - \mu_{\text{NaCl}, v}^0 = RT \ln a_{\text{NaCl}, v}, \quad (2)$$

calculated for the experimental P-T parameters are reported in Table 2. Since the solubility values in our experiments are very low, the concentration dependence of NaCl activity in gaseous CO₂ was described using Darken’s quadratic formalism (DQF) [26–28], according to which

$$RT \ln a_{\text{NaCl}, v} = RT \ln x_{\text{NaCl}, v} + W_{\text{NaCl}-\text{CO}_2}^G \times x_{\text{NaCl}, v} (x_{\text{NaCl}, v} - 2) + B_{\text{NaCl}-\text{CO}_2}^G, \quad (3)$$

where $x_{\text{NaCl}, v}$ is the molar fraction of NaCl in the gaseous phase and $W_{\text{NaCl}-\text{CO}_2}^G$ and $B_{\text{NaCl}-\text{CO}_2}^G$ are empirical constants. Considering that, at very low $x_{\text{NaCl}, v}$ values in our experiments, $(x_{\text{NaCl}, v} - 2) \approx -2$, Eq. (3) can be transformed into

$$RT \ln a_{\text{NaCl}, v} = RT \ln x_{\text{NaCl}, v} - 2W_{\text{NaCl}-\text{CO}_2}^G x_{\text{NaCl}, v} + B_{\text{NaCl}-\text{CO}_2}^G. \quad (3')$$

The temperature and pressure dependences of the parameters of Eqs. (3) and (3') can be expressed using the Gibbs–Duhem relation [26] as

$$\begin{aligned} W^G &= W^H - TW^S + PW^V \\ B^G &= B^H - TB^S + PB^V. \end{aligned} \quad (4)$$

The numerical values of parameters in Eqs. (3) and (4) were found by processing experimental data by the technique of least squares. As it turned out in the course of the calculations, the temperature terms in (4) can be neglected, and four parameters are sufficient for the adequate description of the experiments by the DQF model

$$\begin{aligned} W_{\text{NaCl}-\text{CO}_2}^G &= (1936.3 - 43.669P)10^6 \\ B_{\text{NaCl}-\text{CO}_2}^G &= 83754 - 420.1P. \end{aligned}$$

The DQF model is able to very well fit the experimentally measured values of NaCl solubility (solid lines in Fig. 1), but extrapolations with this model should be carried out very cautiously because of the very narrow P–T–X ranges of our experiments

MIXING PROPERTIES IN THE BINARY SYSTEM H₂O–NaCl AT HIGH P–T PARAMETERS

A simple empirical model was suggested in [1, 24] for the description of H₂O and NaCl activities in the binary system at high temperatures and pressures ($T \geq 773$ K, $P \geq 200$ MPa)

$$\begin{aligned} RT \ln a_{\text{H}_2\text{O}} &= RT \ln X_{\text{H}_2\text{O}} \\ &- RT \ln(1 + \alpha X_{\text{H}_2\text{O}}) + W_2 X_{\text{NaCl}}^2, \end{aligned} \quad (5)$$

$$\begin{aligned} RT \ln a_{\text{NaCl}} &= (1 + \alpha)RT[\ln X_{\text{NaCl}} \\ &- \ln(1 + \alpha X_{\text{NaCl}}) + \ln(1 + \alpha)] + W_2 X_{\text{NaCl}}^2. \end{aligned} \quad (6)$$

In Eqs. (5) and (6), α and W_2 are empirical parameters dependent on T and P

$$\alpha = \exp(4.04 - 0.161V_1) - 134.2 \cdot P/T, \quad (7)$$

$$W_2 = 906.12 - 57.277P, \quad (7')$$

where P is expressed in bar, T is in K, and $V_1 = V_{\text{H}_2\text{O}}$ is the molar volume of pure water (cm³/mol) at corresponding T and P .

The numerical values of the parameters were obtained by the thermodynamic treatment of experimental data on the equilibrium conditions of the brucite dehydration reaction in the presence of an aqueous salt fluid [1, 24]. As was demonstrated in [1], the MgO solubility in this fluid is very low and can be neglected in the analysis of activity–composition relations in the pure binary system. Conversely, the silica

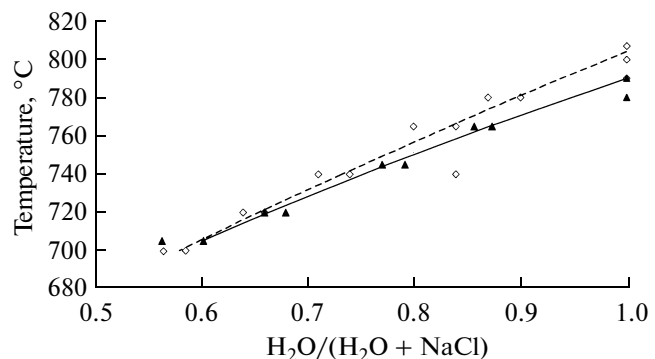


Fig. 2. Comparison of experimental data on equilibrium (A) (see text and Table 3) with calculations by model [1, 24].

Diamonds and triangles are experimental data, curves are calculations at 1000 MPa (dashed line) and 700 MPa (continuous line).

solubility in the fluid is fairly high [29, 30], and theoretically, this can result in appreciable deviations of $a_{\text{H}_2\text{O}}$ in silica-rich chloride solutions from values calculated for true binary fluids. In order to quantify this effect, we examined the equilibrium conditions of the talc dehydration reaction



in the presence of H₂O–NaCl fluid. The experiments at 700 and 1000 MPa were conducted in a piston–cylinder apparatus, in NaCl cells with a graphite heater. The experimental techniques are described in detail in [1, 24]. In each experiment, the cells contained two Pt ampoules with the starting mixtures of synthetic talc, enstatite (the reader can find the conditions under which they were synthesized and their characteristics in [31]), and natural quartz, with their total mass amounting to 5–7 mg, 1–2 mg of distilled H₂O, and a certain amount of NaCl (of analytical-grade purity), which was preliminarily calcined at 350°C. The composition of the fluid [its $X_{\text{NaCl}} = \text{NaCl}/(\text{NaCl} + \text{H}_2\text{O})$ ratio] in the pairs of ampoules was chosen in such a manner that reaction (A) proceeded from its left- to the right-hand part in one of the ampoules and in the opposite direction in the other; i.e., the equilibria were bracketed on two sides in terms of fluid composition. The quantitative proportions of minerals usually significantly varied in the products of the paired experiments with the starting fluid components differing as little as 0.03 units of X_{NaCl} .

The experimental results are reported in Table 3 and graphically represented in Fig. 2, in which they are compared with the calculated equilibrium conditions of reac-

Table 3. Experimental data on the reaction $Tc = 3En + Qz + H_2O$ in H_2O -NaCl solutions

Experiment. no.	$T^\circ C$	X_{H_2O}	Stable phases	Reaction yield
$P = 1000 \text{ MPa}$				
TEQ-11	800	1	$En + Qz$	Insignificant
TEQ-12	790	1	Tc	Significant
TEQ-57	780	0.88	$En + Qz$	Significant
TEQ-58	780	0.91	Tc	Significant
TEQ-37	765	0.8	$En + Qz$	Very insignificant
TEQ-38	765	0.86	Tc	100%
TEQ-43	765	0.78	$En + Qz$	Significant
TEQ-44	765	0.77	$En + Qz$	100%
TEQ-50	765	0.83	Tc	Insignificant
TEQ-51	765	0.79	$En + Qz$	Significant
TEQ-27	740	0.84	Tc	100%
TEQ-28	740	0.69	$En + Qz$	100%
TEQ-30-1	740	0.77	Tc	Significant
TEQ-30-2	740	0.74	Tc	Insignificant
TEQ-33	740	0.71	$En + Qz$	Moderate
TEQ-55	720	0.64	$En + Qz$	Insignificant
TEQ-56	720	0.67	Tc	Moderate
TEQ-31	700	0.5	$En + QZ$	Significant
TEQ-32	700	0.59	$En + Qz$	Significant
TEQ-35	700	0.62	Tc	Significant
$P = 700 \text{ MPa}$				
TEQ-45	790	1	$En + Qz$	Significant
TEQ-42	780	1	Tc	Moderate
TEQ-59	765	0.83	$En + Qz$	100%
TEQ-60	765	0.85	$En + Qz$	Very insignificant
TEQ-67	765	0.86	Tc	Moderate
TEQ-68	765	0.88	Tc	Significant
TEQ-79	745	0.75	$En + Qz$	Moderate
TEQ-80	745	0.78	Tc	Significant
TEQ-61	720	0.7	Tc	100%
TEQ-62	720	0.73	Tc	100%
TEQ-65	720	0.66	$En + Qz$	Moderate
TEQ-66	720	0.68	Tc	Significant
TEQ-63	700	0.65	Tc	Significant
TEQ-64	700	0.68	Tc	100%
TEQ-69	700	0.63	Tc	Significant
TEQ-70	700	0.61	Tc	Significant
TEQ-73	700	0.56	$En + Qz$	Moderate
TEQ-74	700	0.59	Tc	Significant
TEQ-71	660	0.57	Tc	Significant
TEQ-72	660	0.53	Tc	Significant

Note: The reaction yield was evaluated from the change in the height of the X-ray diffraction reflections and from the comparison of the experimental products and starting materials in immersion liquids.

tion (A). At the experimental P – T parameters, these conditions are expressed as

$$\Delta G_{1,T}^0(A) + \int_1^P (\Delta V_s(A)) dP + RT \ln f_{H_2O}^0(P, T) + RT \ln a_{H_2O} = 0. \quad (8)$$

In Eq. (8), $\Delta G_{1,T}^0(A)$, and $\Delta V_s(A)$ are the Gibbs free energy and volume difference of solid phases in reaction (A); and $f_{H_2O}^0(P, T)$ is the fugacity of pure H₂O.

The values of these terms were calculated using the thermodynamic database [25], because, as was demonstrated in [31], these data very closely reproduce the experimental curve for reaction (A) in pure water up to a pressure of 2000 MPa. The value of the last summand in (8) was calculated using (5) and parameters from (7) and (7'). The very good agreement of the calculated and experimental results (Fig. 2) testifies that the model suggested in [1, 24] for H₂O activity can be readily employed to calculate mineral reactions in the presence of a fluid of H₂O–alkali haloids, or, at least those for which no significant salting-out effect is expected (for example, this effect in reactions with calcite is very significant [32]).

MIXING PROPERTIES IN THE TERNARY SYSTEM H₂O–CO₂–NaCl

Preparatorily to proceeding to the description of the mixing properties of the ternary system, it is pertinent to briefly dwell on the last of the boundary binary system: H₂O–CO₂. Its Gibbs free energy was described in [31] with the application of the Van Laar equations with parameters calibrated against experimental data on the equilibrium conditions of simple dehydration and decarbonatization reactions. Later Holland and Powell [33] suggested a somewhat simpler form of the Van Laar equation and demonstrated that it almost exactly corresponds to experimental data [31]. With regard to this result, an equation for the integral excess Gibbs energy for the system H₂O–CO₂ assumes the form

$$G^{ex} = W_1 X_1 X_2 / (V_1 X_1 + V_2 X_2). \quad (9)$$

In (9), X_1 and X_2 are the molar fractions of H₂O and CO₂; V_1 and V_2 are their standard molar volumes (cm³/mol) at corresponding P and T ; and W_1 is an empirical parameter, whose values was calculated from experimental data [31]

$$W_1 = 202046 \text{ (J cm}^3/\text{mol}). \quad (9')$$

An expression for the integral Gibbs free energy (G^{mix}) of the ternary system H₂O–CO₂–NaCl was obtained as a linear combination of equations for the boundary binary systems with the addition of a term that takes into account

the interaction of all three components [the last summand, which includes the parameter W_5 in Eq. (10)]

$$\begin{aligned} G^{mix} = & RT(X_1 \ln X_1 + X_2 \ln X_2 + X_3 \ln X_3) \\ & + W_1 X_1 X_2 (X_1 + X_2) / (V_1 X_1 + V_2 X_2) + X_1 X_3 W_2 \\ & - X_1 R T \ln [1 + \alpha X_3 / (X_1 + X_3)] + X_3 R T \{ (1 + \alpha) \\ & \times \ln (1 + \alpha) + \alpha \ln [X_3 / (X_1 + X_3)] - (1 + \alpha) \\ & \times \ln [1 + \alpha X_3 / (X_1 + X_3)] \} + X_2 X_3 \\ & \times (X_2 W_3 + X_3 W_4) / (X_2 + X_3) + X_1 X_2 X_3 W_5. \end{aligned} \quad (10)$$

In Eq. (10), X_1 , X_2 , and X_3 are the molar fractions of H₂O, CO₂, and NaCl, respectively ($\sum X_i = 1$); and W_1 , W_2 , V_1 , V_2 , and α — are parameters whose values were presented and the sense was explained above. To describe the binary system CO₂–NaCl over an as much as possible broad compositional range, we applied a model of subregular solution [summands with W_3 and W_4 in (10)] instead of Eq. (3). The numerical values of parameters W_3 , W_4 , and W_5 were calculated at the simultaneous processing of experimental results from Table 2 and those on the boundaries of the field of homogeneous H₂O–CO₂–NaCl fluid obtained by studying synthetic fluid inclusions in quartz [9, 10, 34]

$$\begin{aligned} W_3 &= 101788 - 29.16 P, \\ W_4 &= 38007 + 24.45 P, \\ W_5 &= -37371 + 9.16 P. \end{aligned} \quad (11)$$

Expressions for the activities of components of ternary fluid were derived from (10) with the use of the Gibbs–Duhem relation (Appendix).

In Fig. 3, the calculation results by Eq. (10) with parameters according to (7), (9), and (11) are compared with the results obtained by Frantz [34] (Fig. 3a) and Shmulovich and Graham [9] (Fig. 3b). It can be seen that the calculation results are in good agreement with the reference experimental data. These figures also clearly display the most important topological features of isobaric–isothermal sections of the ternary system at high temperatures and pressures. The petrologically most important issue is the existence of a broad compositional region within which two fluids (\pm salt) can be in equilibrium: an aqueous salt fluid with a low concentration of CO₂ and a CO₂-dominant fluid with a very low concentration of dissolved salt. The slope of the tie lines (thin continuous lines in Fig. 3) is notably more gentle than that according to calculations in [17], i.e., our data testify to much more significant differences between the compositions of the coexisting fluids, first of all, in their H₂O and CO₂ concentrations. The main reason for this is the greater deviations of the boundary binary systems H₂O–CO₂ and H₂O–NaCl from ideality. An important consequence of the nonideality of component mixing in the ternary fluid is the significant difference in the location of the equilibrium lines of dehydration and decarbonatization reactions in the ternary system compared to those in the binary system H₂O–CO₂. As an example, Fig. 4 shows

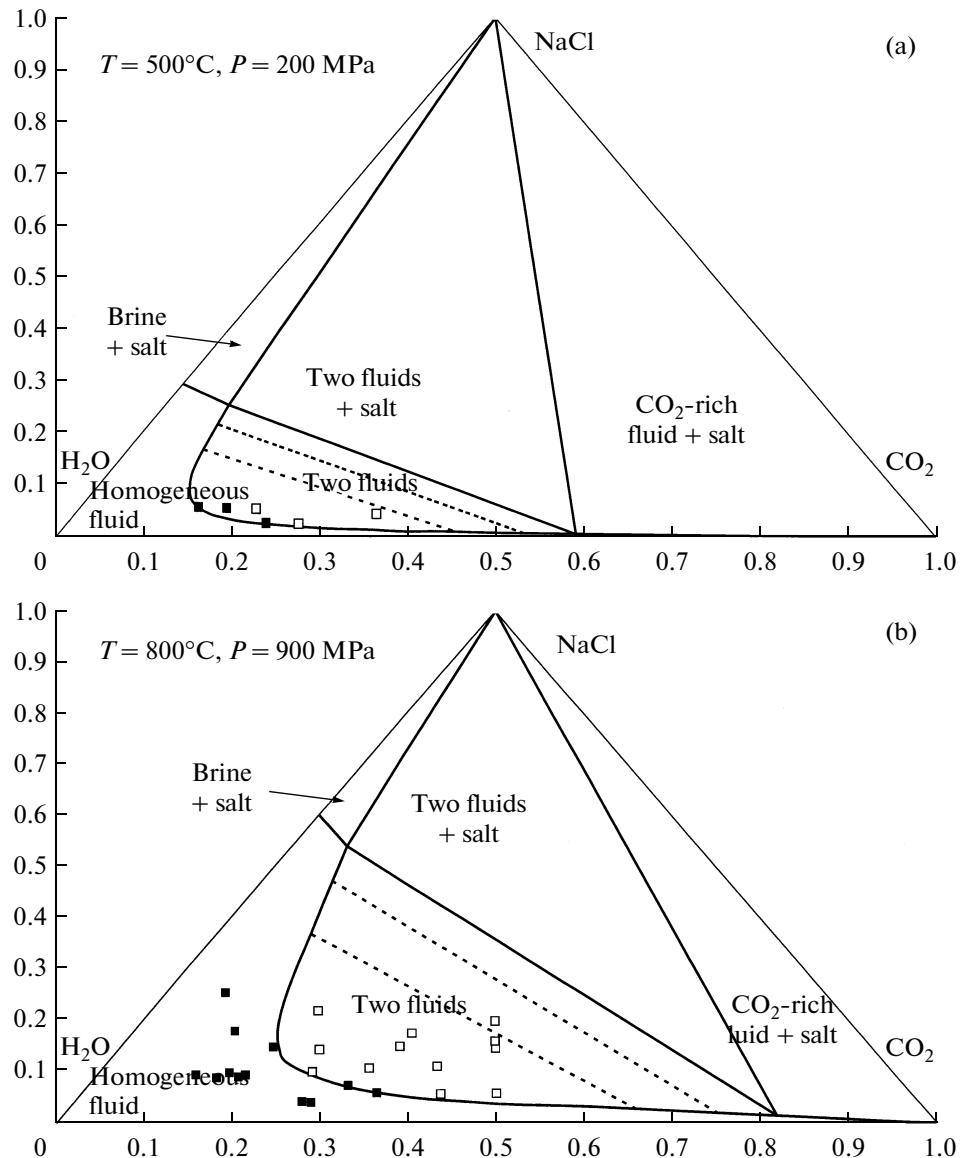
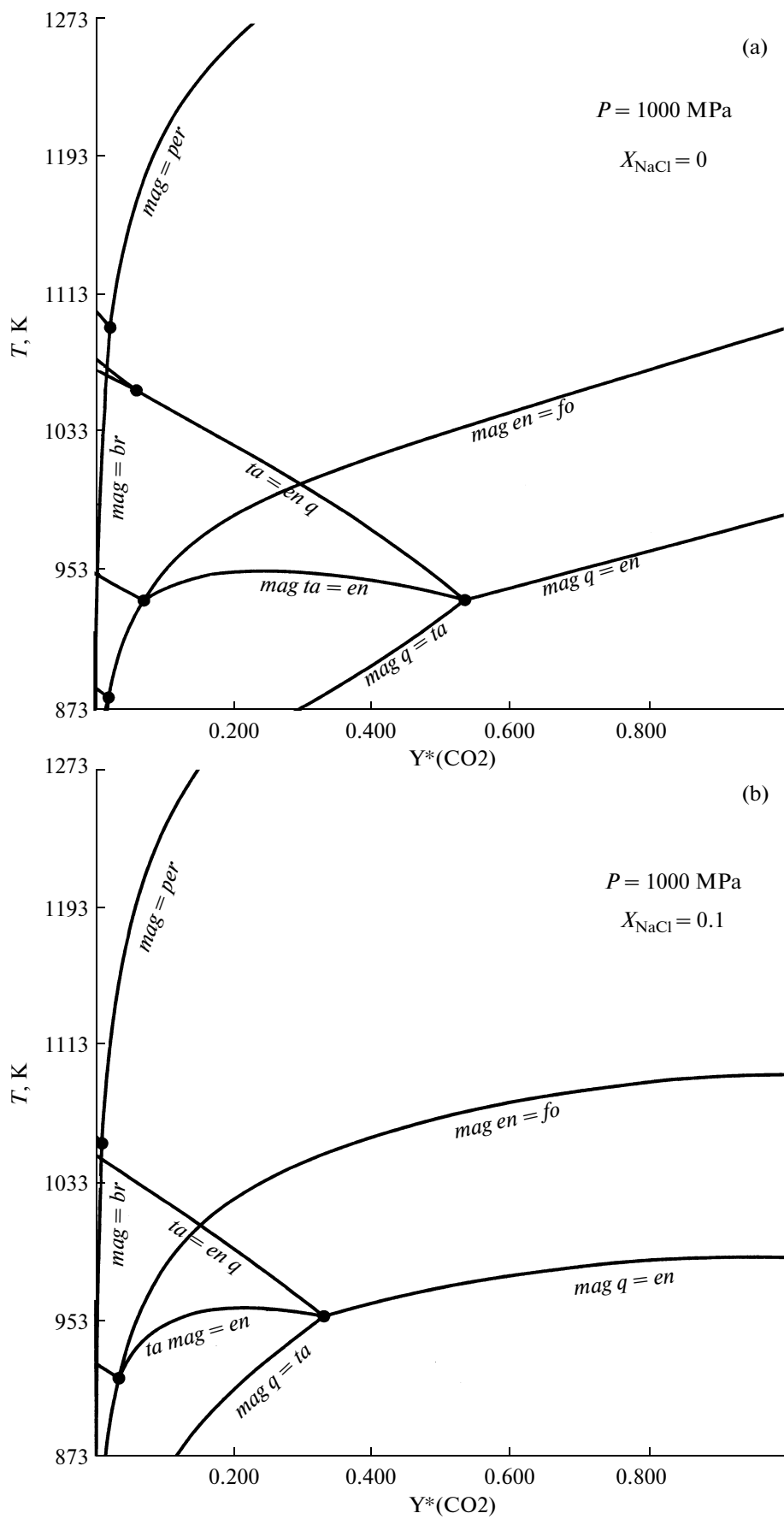


Fig. 3. Calculated phase diagrams for the ternary system $\text{H}_2\text{O}-\text{CO}_2-\text{NaCl}$ (heavy continuous lines in the compositional triangle) in comparison with experimentally determined boundaries of the homogeneity region (solid squares are homogeneous fluid, open squares are two-phase fluid). Experiments at 500°C , 200 MPa (Fig. 3a) [34] and 800°C , 900 MPa (Fig. 3b) [9]. Dashed lines show tie lines of coexisting fluids.

calculated curves for isobarically ($P = 1000 \text{ MPa}$) monovariant mineral equilibria in the system $\text{MgO}-\text{SiO}_2-\text{H}_2\text{O}-\text{CO}_2 (\pm \text{NaCl})$ in the presence of binary $\text{H}_2\text{O}-\text{CO}_2$ ($X_{\text{NaCl}} = 0$) (Fig. 4a) and ternary ($X_{\text{NaCl}} = 0.1$) (Fig. 4b) fluids. The addition of salt notably shifts the monovariant reactions and corresponding invariant points toward lower $\text{CO}_2/(\text{H}_2\text{O} + \text{CO}_2)$ ratios. Because of this, evaluations of the composition of a metamorphic fluid based on

the calculation of mineral equilibria in intercalating aluminosilicate and calc-silicate rocks under the assumption of binary $\text{H}_2\text{O}-\text{CO}_2$ fluid can involve significant errors if the fluid contained a certain amount of a strong electrolyte. With regard to the possible salt content, the paths of decarbonatization reactions in calc-silicate rocks can also notably change [12].

Fig. 4. Isobaric ($P = 1000 \text{ MPa}$) sections of a phase diagram for the system $\text{MgO}-\text{SiO}_2-\text{H}_2\text{O}-\text{CO}_2 (\pm \text{NaCl})$ (a) in the absence of salt and (b) at a salt concentration in the fluid $X_{\text{NaCl}} = 0.1$. The ordinate corresponds to the $Y^*(\text{CO}_2) = \text{CO}_2/(\text{H}_2\text{O} + \text{CO}_2)$ ratio. Mineral symbols: *br* — brucite, *en* — enstatite, *fo* — forsterite, *mgs* — magnesite, *per* — periclase, *q* — quartz, and *tc* — talc. The calculations were carried out using thermodynamic constants from [25] and equations of component activities from this publication.



ACKNOWLEDGMENTS

This study was supported by the Russian Foundation for Basic Research (project nos. 09-05-00193, 07-05-92105-GFEN) and programs 4 and 7 of the Earth Science Division, Russian Academy of Sciences.

APPENDIX. EQUATION FOR THE ACTIVITIES OF COMPONENTS IN THE TERNARY FLUID ACCORDING TO THE MIXING MODEL (10)

Expressions for the activities of components of the ternary fluid were derived from (10) using the Gibbs–Duhem relation, which is written for multicomponent solutions as [28]

$$G_i^{mix} = RT \ln a_i = G^{mix} - \sum_{k \neq i}^c \left[\frac{\partial G^{mix}}{\partial X_k} \right]_{T, P, x_j \neq i, k} X_k.$$

Upon differentiating and canceling similar terms, we arrive at

$$\begin{aligned} G_1^{mix} &= RT(\ln X_1 - \ln[1 + X_3\alpha/(X_1 + X_3)]) + W_2 X_3 (X_1 \\ &+ X_3) - X_2 X_3 (W_3 X_2 + W_4 X_3)/(X_2 + X_3) + W_1 X_2 (V_1 X_1^2 X_3 \\ &+ V_2 X_2 (X_1 + X_2 + X_1 X_3))/(V_1 X_1 + V_2 X_2)^2 - W_5 X_2 (X_1 - X_2 \\ &- X_3) X_3; \end{aligned}$$

$$\begin{aligned} G_2^{mix} &= RT \ln X_2 - W_2 X_1 X_3 + W_5 X_1 X_3 (X_1 - X_2 + X_3) \\ &+ W_1 X_1 (V_2 X_2^2 X_3 + V_1 X_1 (X_1 + X_2 + X_2 X_3))/(V_1 X_1 + V_2 X_2)^2 \\ &+ (X_3/(X_2 + X_3))^2 (W_4 X_3 (X_1 X_3 + X_3^2 - X_2^2) + W_3 X_2 (2 X_3 (X_2 \\ &+ X_3) + X_1 (X_2 + 2 X_3))); \end{aligned}$$

and

$$\begin{aligned} G_3^{mix} &= RT(\ln X_3 + \alpha \ln[X_3/(X_1 + X_3)] + (1 + \alpha)(\ln[1 \\ &+ \alpha] - \ln[1 + X_3\alpha/(X_1 + X_3)])) + W_2 X_1 (X_1 + X_2) \\ &- W_1 X_1 X_2 (X_1 + X_2)/(V_1 X_1 + V_2 X_2) + W_5 X_1 X_2 (X_1 + X_2 \\ &- X_3) + X_2 (W_3 X_2 (X_1 X_2 + X_2^2 - X_3^2) + W_4 X_3 (2 X_2 (X_2 \\ &+ X_3) + X_1 (2 X_2 + X_3)))/(X_2 + X_3)^2. \end{aligned}$$

All symbolism in these equations is the same as in (10).

REFERENCES

1. L. Y. Aranovich and R. C. Newton, "H₂O Activity in Concentrated KCl and KCl–NaCl Solutions at High Temperatures and Pressures Measured by the Brucite–Periclase Equilibrium," *Contrib. Mineral. Petrol.* **127**, 261–271 (1997).
2. D. S. Korzhinskii, "Principle of Alkali Mobility during Magmatic Phenomena," in *On the 70th Anniversary of the Academician D.S. Belyankin* (Akad. Nauk SSSR, Moscow, 1946), pp. 134–152 [in Russian].
3. D. S. Korzhinskii, *Physicochemical Principles of Paragenetic Analysis of Minerals* (Akad. Nauk SSSR, Moscow, 1957) [in Russian].
4. L. Ya. Aranovich, K. I. Shmulovich, and V. V. Fed'kin, "H₂O and CO₂ Regime during Regional Metamorphism," in *Contributions to Physicochemical Petrology* (Nauka, Moscow, 1987), No. 14, pp. 96–117 [in Russian].
5. L. L. Perchuk and T. V. Gerya, "Fluid Control of Charnocitization," *Chem. Geol.* **108**, 175–186 (1993).
6. R. C. Newton, L. Y. Aranovich, E. C. Hansen, and B. A. Vandenheuvel, "Hypersaline Fluids in Precambrian Deep-Crustal Metamorphism," *Precambrian Res.* **38**, 21–34 (1998).
7. J. J. Ague, "Fluid Infiltration and Transport of Major, Minor and Trace Elements during Regional Metamorphism of Carbonate Rocks, Wepawaug Schist, Connecticut, USA," *Am. J. Sci.* **303**, 753–816 (2003).
8. A. R. Kotel'nikov and Z. A. Kotel'nikova, "Experimental Study of the Phase State of the H₂O–CO₂–NaCl System by the Method of Synthetic Quartz Inclusions in Quartz," *Geokhimiya*, No. 4, 526–537 (1990).
9. K. I. Shmulovich and C. M. Graham, "An Experimental Study of Phase Equilibria in the System H₂O–CO₂–NaCl at 800°C and 9 Kbar," *Contrib. Mineral. Petrol.* **136**, 247–257 (1999).
10. K. I. Shmulovich and C. M. Graham, "An Experimental Study of Phase Equilibria in the Systems H₂O–CO₂–CaCl₂ and H₂O–CO₂–NaCl at High Pressures and Temperatures (500–800°C, 0.5–0.9 GPa): Geological and Geophysical Applications," *Contrib. Mineral. Petrol.* **146**, 450–462 (2004).
11. G. Skippen and V. Trommsdorff, "The Influence of NaCl and KCl on Phase Relations in Metamorphosed Carbonate Rocks," *Am. J. Sci.* **286**, 81–104 (1986).
12. W. Heinrich, S. S. Churakov, and M. Gottschalk, "Mineral–Fluid Equilibria in the System CaO–MgO–SiO₂–H₂O–CO₂–NaCl and the Record of Reactive Fluid Flow in Contact Metamorphic Aureoles," *Contrib. Mineral. Petrol.* **148**, 131–149 (2004).
13. V. Trommsdorff, G. Skippen, and P. Ulmer, "Halite and Sylvite as Solid Inclusions in High-Grade Metamorphic Rocks," *Contrib. Mineral. Petrol.* **89**, 24–29 (1985).
14. G. Markl and K. Bucher, "Composition of Fluids in the Lower Crust Inferred from Metamorphic Salt in Lower Crustal Rocks," *Nature* **391**, 781–783 (1998).
15. K. I. Shmulovich, *Carbon Dioxide in High-Temperature Mineral-Forming Processes* (Nauka, Moscow, 1988) [in Russian].
16. I. V. Zakirov and N. G. Sretenskaya, "Technique of Experimental Determination of Phase Composition under Heterogeneous Conditions," in *Experimental Problems of Geology* (Nauka, Moscow, 1994), pp. 664–667 [in Russian].
17. Z. Duan, N. Moller, and J. H. Weare, "Equation of State for the NaCl–H₂O–CO₂ System: Prediction of Phase Equilibria and Volumetric Properties," *Geochim. Cosmochim. Acta* **59**, 2869–2882 (1995).
18. K. Grjotheim, P. Heggelund, C. Krohn, and K. Motzfeldt, "On the Solubility of Carbon Dioxide in Molten Halides," *Acta Chem. Scandinav.* **16**, 689–694 (1962).
19. I. M. Chou, "Halite Solubilities in Supercritical Carbon Dioxide–Water Fluids," *GSA Abstracts with Programs* **20** (7), 76 (1988).
20. T. S. Bowers and H. C. Helgeson, "Calculation of the Thermodynamic and Geochemical Consequences of Nonideal Mixing in the System H₂O–CO₂–NaCl on Phase Relations in Geologic Systems: Equation of State for

- H₂O–CO₂–NaCl Fluids at High Pressures and Temperatures,” *Geochim. Cosmochim. Acta* **47**, 1247–1275 (1983).
21. I. V. Zakirov, N. G. Sretenskaja, L. Y. Aranovich, and V. A. Volchenkova, “Solubility of NaCl in CO₂ at High Pressure and Temperature: First Experimental Measurements,” *Geochim. Cosmochim. Acta* **71**, 4251–4255 (2007).
22. L. V. Gurvich, I. V. Veits, V. A. Medvedev, et al., *Thermodynamic Properties of Substances* (Nauka, Moscow, 1978), Vol. 1, Book 1.
23. I.-M. Chou, S. M. Sterner, and K. S. Pitzer, “Phase Relations in the System NaCl–KCl–H₂O: IV. Differential Thermal Analysis of the Sylvite Liquidus in the KCl–H₂O Binary, the Liquidus in the NaCl–KCl–H₂O Ternary, and the Solidus in the NaCl–KCl Binary to 2 Kb Pressure, and a Summary of Experimental Data for Thermodynamic PTX-Analysis of Solid–Liquid Equilibria at Elevated P–T Conditions,” *Geochim. Cosmochim. Acta* **56**, 2281–2293 (1992).
24. L. Y. Aranovich and R. C. Newton, “H₂O Activity in Concentrated NaCl Solutions at High Pressures and Temperatures Measured by the Brucite–Periclase Equilibrium,” *Contrib. Mineral. Petrol.*, 200–212 (1996).
25. T. J. B. Holland and R. Powell, “An Internally Consistent Thermodynamic Data Set for Phases of Petrological Interest,” *J. Metamorph. Geol.* **16**, 309–343 (1998).
26. L. S. Darken, “Thermodynamics of Binary Metallic Solutions,” *Trans. Metal. Soc. AIME* **239**, 80–89 (1967).
27. V. V. Slavinskii, Candidate’s Dissertation in Geology and Mineralogy (Moscow, 1976).
28. L. Ya. Aranovich, *Mineral Equilibria of Multicomponent Solutions* (Nauka, Moscow, 1991) [in Russian].
29. R. C. Newton and C. E. Manning, “Quartz Solubility in H₂O–NaCl and H₂O–CO₂ Solutions at Deep Crust–Upper Mantle Pressures and Temperatures: 2–15 Kbar and 500–900°C,” *Geochim. Cosmochim. Acta* **64**, 2993–3005 (2000).
30. K. I. Shmulovich, C. M. Graham, and B. Yardley, “Quartz, Albite and Diopside Solubilities in H₂O–NaCl and H₂O–CO₂ Fluids at 0.5–0.9 GPa,” *Contrib. Mineral. Petrol.* **141**, 95–108 (2001).
31. L. Y. Aranovich and R. C. Newton, “Experimental Determination of CO₂–H₂O Activity–Composition Relations at 600–1000°C and 6–14 Kbar by Reversed Decarbonation and Dehydration Reactions,” *Am. Mineral.* **84**, 1319–1332 (1999).
32. R. C. Newton and C. E. Manning, “Experimental Determination of Calcite Solubility in H₂O–NaCl Solutions at Deep Crust/Upper Mantle Pressures and Temperatures: Implications for Metasomatic Processes in Shear Zones,” *Am. Mineral.* **87**, 1401–1409 (2002).
33. T. J. B. Holland and R. Powell, “Activity–Composition Relations for Phases in Petrological Calculations: An Asymmetric Multicomponent Formulation,” *Contrib. Mineral. Petrol.* **145**, 492–501 (2003).
34. J. D. Frantz, R. K. Popp, and T. C. Hoering, “The Compositional Limits of Liquid Immiscibility in the System H₂O–NaCl–CO₂ as Determined with the Use of Synthetic Fluid Inclusions in Conjunction with Mass Spectrometry,” *Chem. Geol.* **98**, 237–255 (1992).